Catal Lett (2008) 125:340–347
DOI 10.1007/s10562-008-9570-x

A Highly Effective Pt and $H_3PW_{12}O_{40}$ Modified Zirconium Oxide Metal–Acid Bifunctional Catalyst for Skeletal Isomerization: Preparation, Characterization and Catalytic Behavior Study

Yuandong Xu · Xia Zhang · Hongling Li · Yanxing Qi · Gongxuan Lu · Shuben Li

Received: 22 May 2008 / Accepted: 30 June 2008 / Published online: 16 July 2008

Abstract A series of metal–acid bifunctional catalysts with varying quantities of platinum and tungstophosphoric acid (TPA) supported on zirconium oxide were prepared by co-impregnation method. In skeletal isomerization of n-pentane using catalyst with 1% Pt and 30% TPA loadings the conversion of the reactant which was close to the equilibrium conversion reached ca. 65% and the selectivity towards the product was as high as ca. 97% at atmospheric pressure and relatively low reaction temperature (200 °C). The phase structure, chemical structure, surface physicochemical properties, surface element oxidation states and hydrogen reduction behavior of the catalysts were well-characterized via XRD, FT-IR, N_2 adsorption–desorption determination (BET), XPS and TPR. The effects of Pt and TPA loadings, calcination temperature, reaction temperature and weight hourly space velocity (WHSV) on the catalytic performance were investigated. In addition, a long period catalytic stability test of the catalyst with optimal Pt and TPA loadings was carried out, which indicated that the bifunctional catalyst was in possession of good stability in skeletal isomerization along with high catalytic activity under the experimental conditions.

Y. Xu · X. Zhang · H. Li · Y. Qi (✉) · G. Lu (✉) · S. Li
State Key Laboratory for Oxo Synthesis and Selective Oxidation, Lanzhou Institute of Chemical Physics, Chinese Academy of Sciences, Lanzhou 730000, People's Republic of China
e-mail: qiyx@lzb.ac.cn

G. Lu
e-mail: gxlu@lzb.ac.cn

Y. Xu · X. Zhang · H. Li
Graduate University of the Chinese Academy of Sciences, Beijing 100039, People's Republic of China

Keywords Bifunctional catalyst · Tungstophosphoric acid · Skeletal isomerization · Catalytic stability test

1 Introduction

Branched alkanes are useful as clean high-octane fuels. By way of the process of skeletal isomerization, linear alkanes can be transformed to significant quantities of the corresponding isomers. Currently, the catalysts used commercially for this reaction are bifunctional (metal–acid), mainly, Pt on highly chlorinated alumina and Pt/mordenite [1–3]. The chlorinated alumina-based catalyst allows operation at low temperature (<150 °C), which is thermodynamically advantageous. However, this type of catalyst requires continuous addition of chlorine and is very sensitive to water and sulfur. At the same time, it is highly corrosive and subject to stringent environmental control. Although Pt/mordenite does not have these drawbacks, it is considerably less active and consequently requires higher operating temperature (>260 °C) where thermodynamic constraint results in lower yield of the branched paraffin. Increasingly stringent environmental regulations, and also the desire to achieve high alkane conversion rates at relatively mild temperature contribute to keep an interest to explore the potential isomerization catalysts.

In recent years, solid acid materials such as sulfated zirconia [4–6], tungstated zirconia [7–9] and heteropoly compound [10, 11], exhibiting stronger acid strength than zeolites, have attracted much attention. Solid acid catalysts combined with noble metals are effective for skeletal isomerization of n-alkanes. Among them, systems based on heteropoly compound is most promising [12]. Suzuki et al. [13] observed that $Pd_xH_{3-2x}PW_{12}O_{40}/SiO_2$ catalyzed

n-hexane isomerization in the presence of hydrogen. Na et al. [14, 15] found that an acidic Cs salt of $H_3PW_{12}O_{40}$, namely $Cs_{2.5}H_{0.5}PW_{12}O_{40}$, was very active and selective for the n-butane skeletal isomerization. Besides the application of heteropoly acid salts, heteropoly acids (HPAs), in particular those with Keggin structure H_{8-x} $[X^{x+}$ $M_{12}O_{40}]$ ($X = P^{5+}$ or Si^{4+}, $M = W^{6+}$or Mo^{6+}), which are strong brønsted acids were also extensively used as acid catalysts [16]. However, a serious problem associated with the use of this type of materials as heterogeneous catalysts is their low surface area (5–8 m^2/g). In view of this, the use of HPAs in supported form is preferable because of its high surface area compared to the bulk type. Up to now, supported HPAs catalysts were widely investigated in a series of reactions such as photocatalysis [17, 18] and oxidation reactions [19, 20] etc. Recently, some researchers synthesized supported HPAs catalysts and studied their catalytic behavior for isomerization reaction [12, 21–23]. Nevertheless, compared with the systems based on sulfated zirconia and tungstated zirconia studied in isomerization and supported HPAs investigated in other type reactions, the supported HPAs studied in isomerization is few and inadequate.

In the present contribution, we have made an attempt to synthesize zirconium oxide supported platinum-promoted TPA catalysts by a simple co-impregnation method and n-pentane which is the main component of the light straight run gasoline fraction was chosen as the model compound for the isomerization behavior study.

2 Experimental

2.1 Catalyst Preparation

Zirconium hydroxide was precipitated from an aqueous solution of zirconium oxychloride by addition of aqueous ammonium hydroxide up to $pH = 9 \pm 0.1$, then washed and dried at 110 °C overnight. Zirconium oxide was obtained by way of calcination of the zirconium hydroxide at 650 °C for 3 h. Platinum promoted TPA/ZrO_2 catalyst was prepared from hexachloroplatinic acid and TPA mixture aqueous solution and zirconium oxide via co-impregnation method as follows: zirconium oxide in powder was dispersed in the mixture aqueous solution under vigorous stirring at room temperature for 70 min. After the solvent was removed with water bath the resulting material was dried at 110 °C. Then the process was followed by calcination in air at different temperatures (200 °C, 300 °C, 400 °C and 500 °C) for 5 h. The catalyst obtained was designated generally as PTZ. In more detail, the catalysts calcined at different temperatures were denoted as PTZ200, PTZ300, PTZ400 and PTZ500, respectively. Platinum-free and TPA-free catalysts (designated as TZ and PZ) were prepared with the same procedure as above except that no Pt or no TPA was added in terms of the requirements. The loadings of Pt and TPA in all the samples were 1% and 30%, respectively, without special explanation.

2.2 Catalyst Characterization

The X-ray diffraction spectra measurements were performed on a Philips Xpert MPD instrument using Cu Kα radiation in the scanning angle range of 5–80° at a scanning rate of 4°/min at 40 mA and 50 kV. FT-IR spectroscopy was carried out on a Bruker IFS 120 FT-IR spectrometer using ca. 0.5 mm KBr pellets containing 2.5% sample. The specific surface area of the catalyst was determined by BET method on a Micromeritics ASAP-2010 apparatus at a liquid nitrogen temperature with N_2 as the absorbent at −196 °C. X-ray photoelectron spectroscopy was carried out using a VG ESCALAB 210 electron spectrometer with Mg Kα radiation. Temperature-programmed reduction analysis (H_2-TPR) was carried out by heating a sample (30 mg) from 25 to 500 °C at 10 °C/min heating rate in a flow of 5 vol% H_2/Ar mixture (40 mL/min). The amount of H_2 consumed was measured by a thermal-conductivity detector.

2.3 Catalytic Performance Evaluation

The catalytic reaction of n-pentane isomerization was carried out in a fixed-bed quartz microtube reactor (8 mm i.d.) under atmospheric pressure. A 0.5 g portion of the catalyst was loaded into the reactor and activated in situ at 200 °C for 90 min in H_2 flow (30 mL/min). The reaction mixture of n-pentane, hydrogen and nitrogen was fed through the catalyst bed and reacted with the required flow rates, respectively. The reaction products were analyzed using an on-line GC 7890 gas chromatograph equipped with a capillary column (plot Al_2O_3/KCl, 30 m × 0.32 mm) connected to a flame ionization detector.

3 Results and Discussion

3.1 Characterization of the Catalyst

Hydrous zirconium oxide support was prepared by a precipitation method via hydrolysis of the zirconium oxychloride under basic condition. After calcination of the resulting hydrous zirconium oxide at 650 °C, zirconium oxide with mixture crystal phase of tetragonal and monoclinic was produced (Fig. 1). The mixed tetragonal and monoclinic phases formed not only in ZrO_2 but also in their supported composites (PZ, TZ and PTZ300). In the tetragonal phase the characteristic 2θ values are at 30.1°

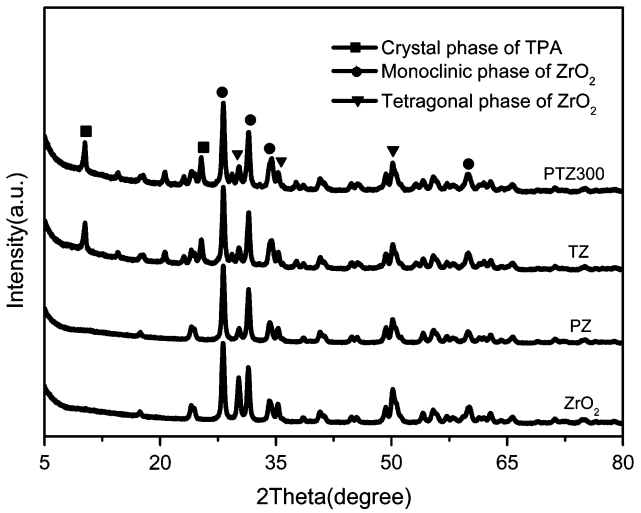

Fig. 1 X-ray diffraction patterns of ZrO_2, PZ, TZ and PTZ300

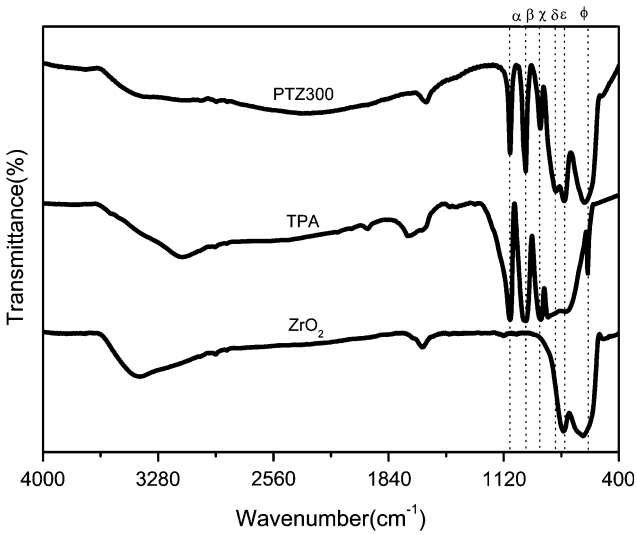

Fig. 2 FT-IR spectra of ZrO_2, TPA and PTZ300

(111), 35.2° (200), 50.4° (220), and 59.9° (311), respectively (JCPDS file 17-0923). The diffraction peaks which locate at 24.0° (011), 28.2° ($\bar{1}11$), 31.4° (111), 34.3° (002), 40.7° ($\bar{2}11$), 44.5° (112), 55.5° (013), and 60.1° ($\bar{3}02$), respectively, correspond to the diffraction of monoclinic ZrO_2 phase (JCPDS file 86-1450). From the XRD patterns it can be seen that the diffraction peak intensity corresponding to T_{111} crystal face of PZ became weaker than that of ZrO_2 and no Pt characteristic diffraction peak was observed. The same phenomena were also found on TZ and PTZ300. The decrease of peak intensity is probably due to the destruction of the T_{111} crystal face during the process of the catalyst preparation and the high dispersion of Pt may be an interpretation to the absence of Pt characteristic diffraction peaks. However, it cannot rule out that the absence of Pt characteristic diffraction peak is resulted from the low loading amount of Pt. In comparison with ZrO_2 other counterpart peaks of zirconium oxide supported composites are all present nearly the same as those from the parent support. Nevertheless, when 30% loading amount of TPA was impregnated onto ZrO_2, TPA characteristic diffraction peaks at $2(\theta) = 10.3°$ and 25.4° [24] were observed, which demonstrated that the crystal structure of TPA was not destroyed after impregnated onto the support.

The infrared spectra of bulk TPA, ZrO_2 and PTZ300 are displayed in Fig. 2. For pure TPA, four characteristic IR absorption peaks in the range from 700 to 1,100 cm^{-1}, corresponding to the stretching vibrations of P–O, W=O, and W–$O_{c/e}$–W bonds of the Keggin units were observed, respectively [22]. Specifically, the peak at ca.1,080 cm^{-1}(α) was originated from the vibration of P–O bonds and the peak at ca. 980 cm^{-1} (β) corresponded to the vibration of W=O bonds and another two peaks at ca. 880 and 800 cm^{-1} (χ and δ) were due to the vibration of two types of W–$O_{c/e}$–W bridge bonds. ZrO_2 showed strong bands at ca. 750 and 630 cm^{-1} (ε and φ), respectively. The supported TPA species were still detected during the FT-IR absorption experiments. Compared to the parent Keggin unit and ZrO_2, the IR peak positions on PTZ300 designated as α, β and χ remained the same as the parent TPA and the other three peaks (δ, ε and ϕ) were the results of the interaction between Keggin units and ZrO_2. The presence of metal particles in interaction with TPA is a subject of controversy with respect to the nature of that interaction. One hypothesis, suggested by CO adsorption studies, is that metal particles interact with the proton of the structure of TPA by forming $(metal–H)^{\delta+}$ species [12]. A second hypothesis is that the particular configuration of hydrogen and oxygen present between TPA proton, water bridge molecules and terminal oxygens from TPA Keggin structure made possible to consider the existence of a noble metal chemical bonding. However, no difference between IR spectra of TPA and TPA-metal (1%) was observed, which may be due to that 1% metal loading is not enough to interact with all the H^+ of TPA structure [25].

Table 1 shows physicochemical properties of the samples of ZrO_2, PZ, TZ and PTZ300 determined by N_2 adsorption–desorption method. After active species were

Table 1 Physicochemical properties of samples

Samples	Pt content (%)	TPA content (%)	S_{BET} (m^2/g)	V_{pore} (cm^3/g)	D_{pore} (nm)
ZrO_2	/	/	30.1	0.217	21.1
PZ	1	/	31.7	0.214	19.0
TZ	/	30	34.8	0.107	8.6
PTZ300	1	30	31.8	0.114	10.3

impregnated onto ZrO_2 the surface area for modified catalysts all increased in comparison with pure ZrO_2. It demonstrated that no obvious pore blocking occurred which may be due to the aggregation of the active species. The change trend of the pore volume is nearly the same as that of the average pore diameter. Generally, the porosity of solids depends not only on the pore size but also on the pores number. Table 1 displays the total pore volume together with the average diameter of the pores, observed on the pore size distribution curves for the samples. It appeared that the highest pore volumes were observed in the case of the pores having relatively large diameters. Thus, the porosity of the studied solids depends essentially on the pore size. That means probably that the number of pores is similar for all the solids and that their sizes influence mainly the pore volume.

The chemical species present on the catalyst surfaces were evaluated by XPS. The results are summarized in Table 2 in terms of the P 2p, W $4f_{7/2}$ and Pt $4f_{7/2}$ binding energies. The energy regions of P 2p, W $4f_{7/2}$ core levels of TPA and P 2p, W $4f_{7/2}$ and Pt $4f_{7/2}$ core levels of PTZ in calcined (300 °C) and reduced (200 °C) samples were recorded, respectively. From the data it can be seen that bulk TPA and the supported one had the same element oxidation states. The observation suggested that after impregnated onto the support and subsequently undergone a series of treatments the surface TPA species still retained the Keggin structure. The corresponding Pt 4f XPS spectra of the two samples are shown in Fig. 3. In this region, both of the original spectra show two peaks. The one at lower binding energy corresponds to Pt $4f_{7/2}$ level and the second one, at higher binding energies, to the Pt $4f_{5/2}$ level. For the two samples treated in different ways there is a clear shift towards lower binding energies for the reduced sample compared to the one that had been only calcined at 300 °C with Pt(IV). The shift corresponds to surfaces dominated by Pt(0) and Pt(II) [26], respectively, which can be seen from the deconvolution of the main peak into two contributions. Moreover, as observed from Table 2, the total XPS surface platinum concentration (given as at.%) of reduced sample decreased compared with that of the calcined one. Such variation might be related to an inward diffusion of Pt.

PTZ300 was also characterized via TPR by increasing temperature until 500 °C (around this temperature TPA starts to decompose irreversibly into phosphorus and tungsten oxides). The TPR profile of PTZ300 is presented in Fig. 4. It is well known that the reduction temperature and hydrogen consumption strongly depend on the nature of the metal. In the TPR curve the first peak is centered at around 100 °C. An additional small reduction peak at around 300 °C and also an important hydrogen consumption peak near to 400 °C were found. The presence of three reduction temperature ranges could be related to the

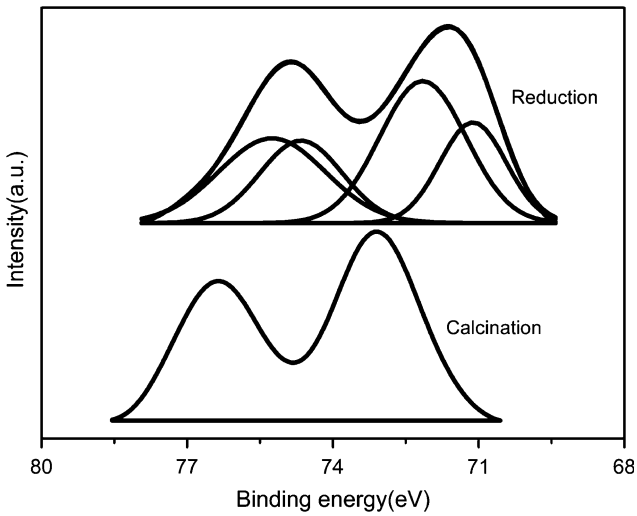

Fig. 3 Pt 4f photoelectron spectra of PTZ calcined at 300 °C and reduced at 200 °C

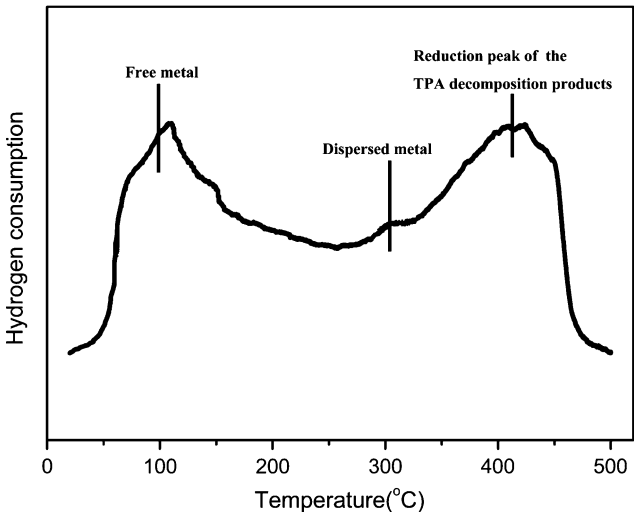

Fig. 4 TPR profile for PTZ300

Table 2 Binding energies of P 2p, W4f and Pt 4f determined by XPS

Samples	Pre-treatment (Temp. °C)	Pt^0 $4f_{7/2}$	$Pt^{II}4f_{7/2}$	Pt (at.%)	P 2p	W $4f_{7/2}$
TPA	Non-treatment	/	/	/	134.1	35.8
PTZ	Calcination (300)	/	73.1	1.08	133.9	35.9
PTZ	Reduction (200)	71.6	/	0.82	134.1	35.9

existence of metal particles in, at least, two different states: free metal and dispersed metal in isolated patches onto the support [27]. The third peak could be attributed to the beginning of TPA structure decomposition (irreversible) into phosphor and tungsten oxides and their subsequent reduction.

3.2 Effect of the Pt and TPA Loadings

The Pt and TPA loadings in the catalysts were varied in the range of 0–1.5% and 0–42%, respectively, and the catalysts were pre-reduced at 200 °C for 90 min and then the reaction started at the same temperature. The activities of the catalysts were determined in terms of conversion of n-pentane and selectivity to iso-pentane as shown in Fig. 5. It is clearly that Pt and TPA loading amount had significant influence on the catalytic performance. During the first 40 minutes the conversions of n-pentane using TZ or PZ catalysts both drastically decreased to below 10% and the corresponding iso-pentane selectivities were also at low values around 80%. Fixing the TPA content at 30% and adding Pt to the catalysts from 0.25% to 1% the conversions of n-pentane gradually increased with the increase of Pt content. Nevertheless, the increase extent of conversion became lower and lower. When the Pt content was below 1% the increase of conversion was evident. Then, adding more Pt to the catalysts its promotion effect to the conversion was negligible. Varying the TPA loading amount from 12% to 42% with a constant Pt content of 1% the conversions of n-pentane were found to reach a steady-state with TPA loading amount above 12%. However, the catalyst with 22% TPA had a relatively long induction period of 60 min. The change of selectivity towards iso-pentane was negligible as soon as Pt and TPA together present in the catalysts and, generally, the selectivity was ca. 97%. According to the experimental results it is evident that the optimal component content should be 1% Pt and 30% TPA. From Fig. 5a, b, we can see that the conversion of n-pentane with TZ or PZ catalysts changed from the maximum values to the low-level steady state. Combined with the corresponding low selectivity of iso-pentane, it is assumed that relatively more hydrogenolysis or cracking reaction occurred. Besides TZ and PZ, the 0.25% and 0.75% Pt content catalysts indicated the same trends according to the conversion curves. It is probably that during the initial reaction period the hydrogenolysis or cracking reaction performed still significantly. Except the conversion curves described before, the rest PTZ300 catalysts all exhibited remarkable increase in activity at the beginning and after tens of minutes the conversion of n-pentane reached stable value. The distribution of side products observed for reaction catalyzed by PTZ300, PZ and TZ in the presence of hydrogen are mainly methane, ethane, propane, iso-butane, n-butane and hexanes. Under

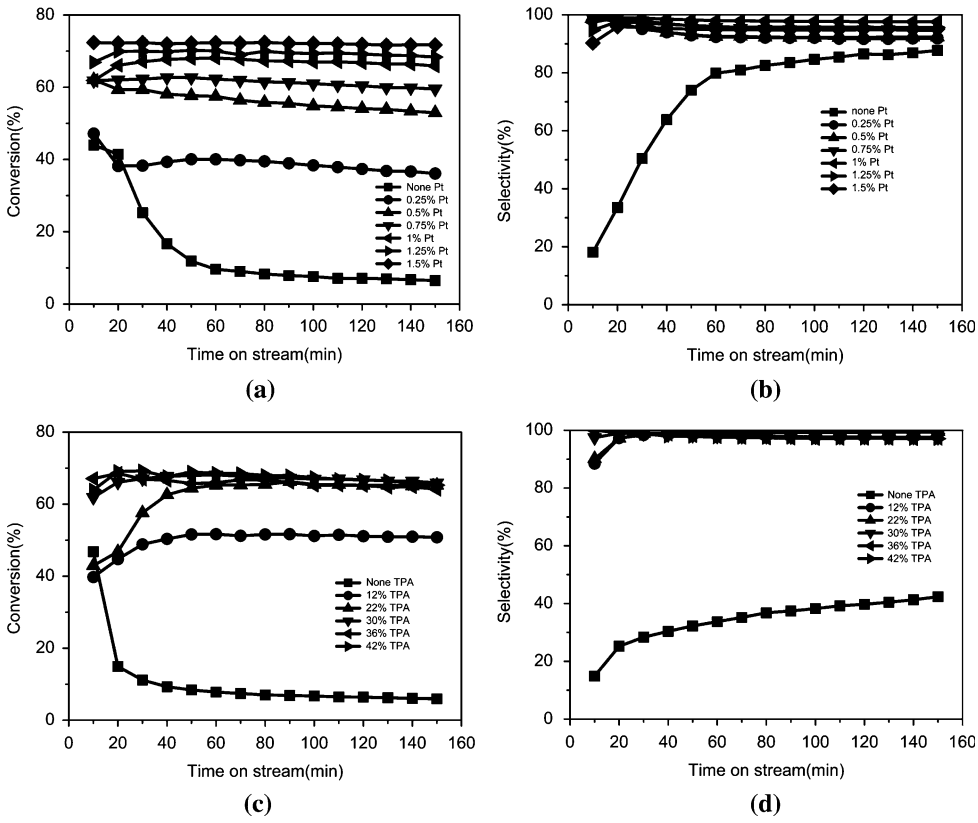

Fig. 5 Effects of Pt and TPA loadings on the catalytic performance of PTZ300 reaction at 200 °C (**a**) effect of Pt loadings with 30% TPA on the conversion; (**b**) effect of Pt loadings with 30% TPA on the selectivity; (**c**) effect of TPA loadings with 1% Pt on the conversion; (**d**) effect of TPA loadings with 1% Pt on the selectivity

Table 3 Product distributions of the skeletal isomerization of n-pentane at different reaction temperatures after reaction for 150 min

Temperature (°C)	Conversion (%)	Selectivity (%)				
		C1–C3	i-C4	n-C4	i-C5	C6
180	51.5	0.08	0.7	0.02	98.4	0.8
200	65.9	0.07	1.3	0.03	97.6	1.0
220	67.9	0.6	4.8	/	90.6	4.0

our experimental conditions the iso-pentane is most probably produced via a monomolecular pathway according to a metal–acid bifunctional mechanism [28]. This involves dehydrogenation of n-pentane to linear pentene on Pt, monomolecular skeletal isomerization of linear pentene with the acid of brønsted acid sites followed by hydrogenation of iso-pentene to iso-pentane on Pt. Nevertheless, it should be noted that bifunctional mechanism is operating parallelly to hydrogenolysis and metal-only isomerization. At the same time, the possibility of dimerization-cracking route to produce iso-pentane can't be totally excluded. It should be then supposed that most of C6 even C7 molecule, which are produced by disproportion of C10 intermediates, are converted to methane and ethane by hydrogenolysis. However, if the dimerization-cracking route took place, non-negligible amounts of C6, and especially higher amounts of propane and butane among the products, are to be expected, which was not the case. From the products distribution listed in Table 3 (200 °C) the main by-products are C4 and C6 and the amount are relatively low, which is a sign of very low dimerization-cracking rate.

3.3 Effect of the Calcination Temperature

The influence of different calcination temperatures (200 °C, 300 °C, 400 °C and 500 °C) on the catalyst activity was investigated. From Fig. 6a it can be seen that the conversion of n-pentane and selectivity of iso-pentane were both increased slightly when the calcination temperature increased from 200 °C to 300 °C. Further increasing the calcination temperature the activity of the catalyst declined drastically. The patterns shown in Fig. 6b revealed that between 200 and 300 °C obvious TPA characteristic diffraction peaks were observed while at higher calcination temperature of 400 and 500 °C the structure of Keggin anions disappeared. The supported TPA samples didn't show diffraction patterns probably due to the following reasons: (i) After treatment at higher temperature, the TPA practically loses its crystalline structure due to the decomposition of the Keggin units; (ii) TPA species were highly dispersed onto the support. However, the catalytic activity of catalysts cancined at higher temperature decreased. So the Keggin anions of TPA decomposed at 400 and 500 °C

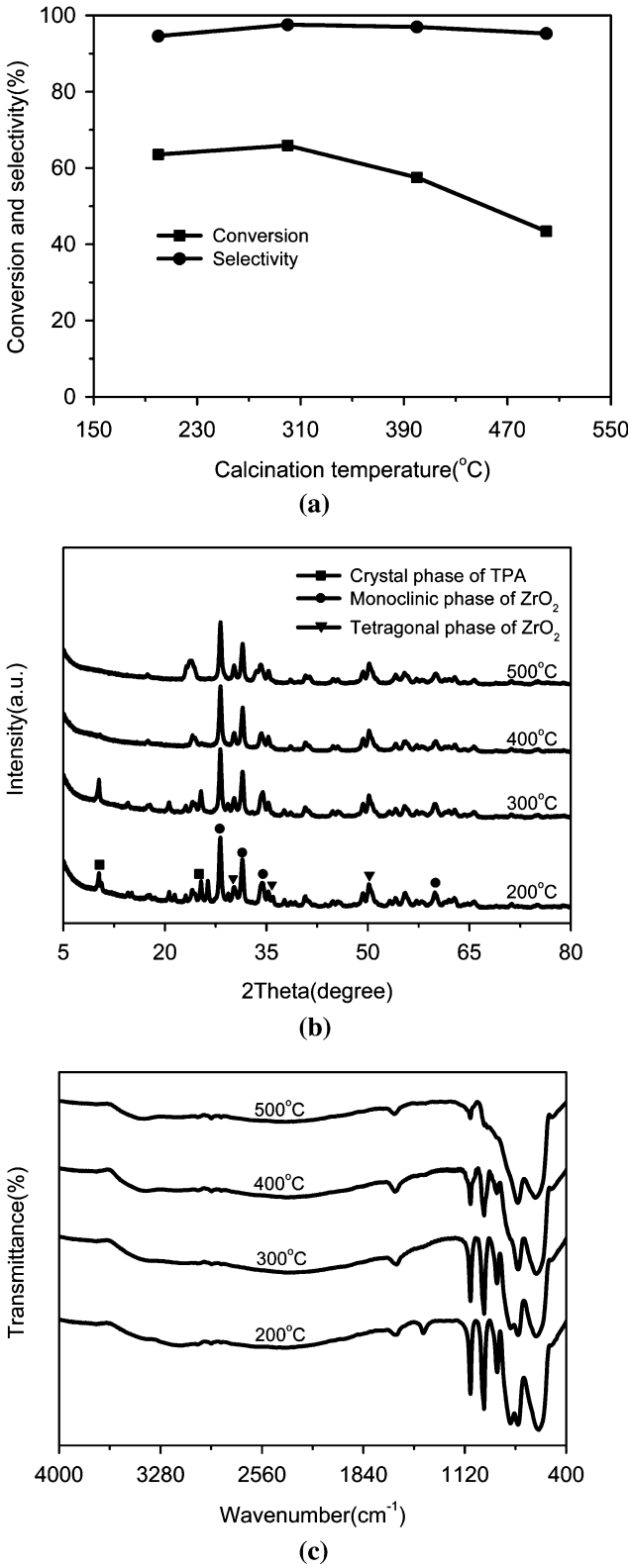

Fig. 6 Effect of calcination temperature on PTZ200, PTZ300, PTZ400 and PTZ500 (**a**) effect of the calcination temperature on the catalytic performance; (**b**) effect of the calcination temperature on the crystal phase; (**c**) effect of the calcination temperature on the FT-IR spectra

may be the real reason. The supported TPA species were however detected during the FT-IR absorption experiments (Fig. 6c). The Keggin structure of TPA calcined at 200, 300 and 400 °C were confirmed by FT-IR spectroscopy. Nevertheless, in comparison with PTZ200 and PTZ300, the IR peak intensity corresponding to TPA on PTZ400 weakened evidently. By way of calcination at 500 °C the IR peaks related to TPA have completely disappeared. Such results are in good agreement with the observation of XRD data. As we all know even low concentration of TPA will generate intensive IR peaks. This further suggested that at higher calcination temperature the Keggin units of TPA were destroyed and as a result a low catalytic activity was observed. It is obvious that with higher calcination temperature, this change trend become more evident. Accordingly, it is concluded that the calcination at different temperatures have obvious influence on the catalytic performance of PTZ catalyst and when the calcination temperature is 300 °C, the catalytic properties maintain the best state.

3.4 Effect of the Reaction Temperature

The effect of the reaction temperature on catalysis is presented in Table 3. It could be observed that reaction temperature had significant influence on the reactant conversion and the product selectivity in the narrow temperature range of 180–220 °C. At 180 °C, the conversion of n-pentane was just 51%, but it reached 65% with the temperature increase to 200 °C. Further increasing the temperature the conversion increased slightly to 67%. On the contrary, the selectivity of iso-pentane decreased appreciably firstly from 98% to 97% and then drastically from 97% to 90% in the range of 180–220 °C. From the data of the products distribution we can see that with the increase of the reaction temperature the content of the by-products, especially i-C4 and C6, increased evidently. The results suggested that improving the reaction temperature was advantageous to the dimerization-cracking reaction which proceeded via β-scission of dimer intermediates (C10) on acid sites and could produce C4 + C6. According to the experimental results, it can be seen that the reaction temperature has significantly influence on the catalytic performance of PTZ300. Very low and too high temperatures are both disadvantageous to the catalytic activity of PTZ type catalyst.

3.5 Effect of the WHSV

The effect of WHSV on skeletal isomerization of n-pentane in the presence of hydrogen over PTZ300 at reaction temperature of 200 °C and $n_{hydrogen}$:$n_{n\text{-}pentane}$ molar ratio of 3:1 was also investigated. Reactant conversion and product selectivity of the reaction at different WHSV (0.24, 0.48 and 0.72 h^{-1}) are shown in Fig. 7. A drastic decrease in n-pentane conversion was observed when the WHSV was increased from 0.24 to 0.72 h^{-1}. The reduction in conversion at higher WHSV may be simply due to the shorter contact time at higher space velocity. The selectivity of iso-pentane was also found to decrease with the increase of WHSV. Usually, a catalyst should be more selective to primary products at lower conversion than it is at higher conversions. However, the change of the selectivities is contrary to the expection. From the product distribution it was found that with the increase of the WHSV the weight percent of C4 and C6 increased slightly. It was suggested that high WHSV may be advantageous to the dimerization-cracking reaction.

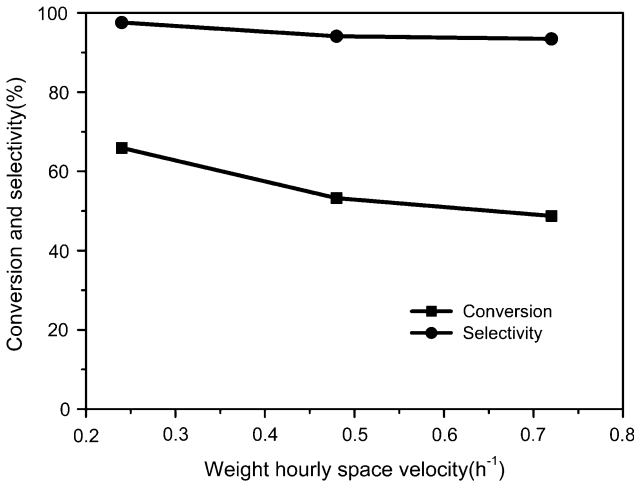

Fig. 7 Effect of the WHSV

3.6 Catalytic Stability Test

Taking into account that Pt promoted TPA catalyst showed better catalytic performance at relatively low temperature of 200 °C, stability test was carried out at this temperature to insight its catalytic behavior thoroughly. The test was performed for 60 h and the results are shown in Fig. 8. The conversion of n-pentane and the selectivity of iso-pentane were plotted as a function of time on stream. In comparison with the initial conversion the terminal conversion had a negligible decrease, while the selectivity towards iso-pentane nearly didn't change during the course. The experimental results indicated that PTZ300 was in possession of good stability in skeletal isomerization along with high catalytic activity under our experimental conditions. As we all know hydrocarbons are easily polymerized to form coke on metal sites, which will make the catalyst lose activity. From the above results we found that PTZ300 catalyst had strong resistance to carbon deposition at the

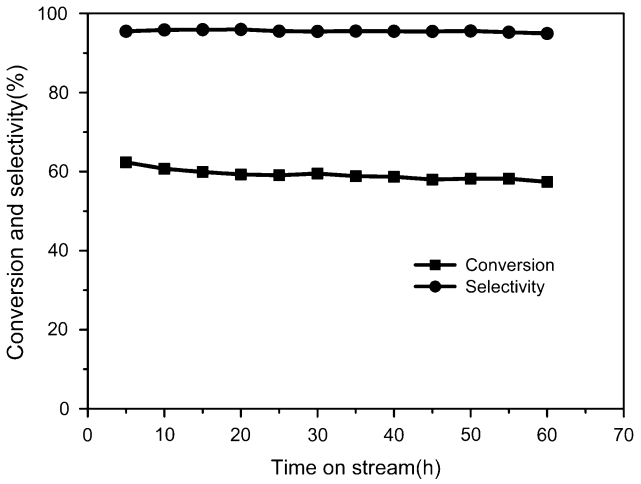

Fig. 8 Stability test for PTZ300 performed at 200 °C

experimental conditions employed. The results indicated that carbon deposition was not serious or the carbon deposition rate was relatively low at the given reaction conditions.

4 Conclusions

Pt–TPA/ZrO_2 with different Pt and TPA loading levels were prepared via co-impregnation method. The composites with 1% Pt and 30% TPA exhibited the best catalytic performance. The conversion of n-pentane was as high as 65% which was nearly amount to the equilibrium conversion. The selectivity of iso-pentane also maintained a high value of 97%. From the analysis of the cracked products, the reaction of skeletal isomerization was typical of a monomolecular metal–acid bifunctional mechanism. XPS results indicated that the surface Pt species calcined at 300 °C was present as Pt(IV) and after reduction at 200 °C for 90 min the valences of Pt became Pt(0) and Pt(II). However, the binding energies of P 2p and W $4f_{7/2}$ remained constant values. It suggested that the Keggin units of supported TPA retained the original state. The effects of different calcination temperatures on the catalytic performance have been investigated. When the calcination temperature was 300 °C, the catalyst exhibited the best catalytic properties. Further increasing the calcination temperature the Keggin units of supported TPA were gradually decomposed. As a result the corresponding catalytic activity decreased drastically. Reaction temperatures in a narrow range from 180 to 220 °C would generate significant influence on the catalytic performance using PTZ300. With the increasing of the reaction temperature more by-products especially C4 and C6 were produced via dimerization-cracking. Varying the WHSV from 0.24 to 0.72 h^{-1} the conversion of the reactant declined rapidly. It is probably due to the reduction of the contact time of the reactant with the catalyst bed. A long period of 60 h stability test of the catalyst was also carried out at 200 °C. During the process the conversion of n-pentane maintained at a relatively high value of about 60% and the selectivity of iso-pentane retained approximately 97%.

References

1. Essayem N, Taarit YB, Feche C, Gayraud PY, Sapaly G, Naccache C (2003) J Catal 219:97
2. Jao RM, Lin TB, Chang JR (1996) J Catal 161:222
3. Wang W, Wang JH, Chen CL, Xu NP, Mou CY (2004) Catal Today 97:307
4. Ahmad R, Melsheimer J, Jentoft FC, Schlögl R (2003) J Catal 218:365
5. Occelli ML, Schiraldi DA, Auroux A, Keogh RA, Davis BH (2001) Appl Catal A Gen 209:165
6. Vijay S, Wolf EE (2004) Appl Catal A Gen 264:117
7. Larsen G, Loteroa E, Raghavana S, Parraa RD, Querini CA (1996) Appl Catal A Gen 139:201
8. Kuba S, Lukinskas P, Ahmad R, Jentoft FC, Grasselli RK, Gates BC, Knözinger H (2003) J Catal 219:376
9. Scheithauer M, Jentoft RE, Gates BC, Knözinger H (2000) J Catal 191:271
10. Moffat JB (1996) Appl Catal A Gen 146:65
11. Miyaji A, Okuhara T (2003) Catal Today 81:43
12. Ivanov AV, Vasina TV, Nissenbaum VD, Kustov LM, Timofeeva MN, Houzvicka JI (2004) Appl Catal A Gen 259:65
13. Suzuki S, Kogai K, Ono Y (1984) Chem Lett 13:699
14. Na K, Okuhara T, Misono M (1993) Chem Lett 22:1141
15. Na K, Okuhara T, Misono M (1995) J Chem Soc Faraday Trans 91:367
16. Kozhevnikov EF, Kozhevnikov IV (2004) J Catal 224:164
17. Qu XS, Guo YH, Hu CW (2007) J Mol Catal A Chem 262:128
18. Guo YH, Hu CW (2007) J Mol Catal A Chem 262:136
19. Ballarini N, Candiracci F, Cavani F, Degrand H, Dubois JL, Lucarelli G, Margotti M, Patinet A, Pigamo A, Trifiro F (2007) Appl Catal A Gen 325:263
20. Predoeva A, Damyanova S, Gaigneaux EM, Petrov L (2007) Appl Catal A Gen 319:14
21. Yori JC, Grau JM, Benitez VM, Sepulveda J (2005) Appl Catal A Gen 286:71
22. Bachiller-Baeza B, Alvarez-Rodriguez J, Guerrero-Ruiz A, Rodriguez-Ramos I (2007) Appl Catal A Gen 333:281
23. Miyaji A, Echizen T, Nagata K, Yoshinaga Y, Okuhara T (2003) J Mol Catal A Chem 201:145
24. Kuang WX, Rives A, Fournier M, Hubaut R (2003) Appl Catal A Gen 250:221
25. Gomez-Garcia MA, Pitchon V, Kiennemann A (2007) Appl Catal B Environ 70:151
26. Neri G, Rizzo G, Arico AS, Crisafulli C, Luca LD, Donato A, Musolino MG, Pietropaolo R (2007) Appl Catal A Gen 325:15
27. Tiernan MJ, Finlayson OE (1998) Appl Catal B Environ 19:23
28. Canizares P, de Lucas A, Dorado F (2000) Appl Catal A Gen 196:225